

Electronic Supplementary Information for:

## Phenylamino Derivatives of Tris(2-pyridylmethyl)amine: Hydrogen-Bonded Peroxodicopper Complexes

Eric W. Dahl, Hai T. Dong, and Nathaniel K. Szymczak\*

### Table of Contents

General Considerations	S2
Experimental Details	S2-S6
<b>Figure S1:</b> $^1\text{H}$ NMR spectrum of $\text{L}^{\text{H}}$	S7
<b>Figure S2:</b> $^{13}\text{C}$ NMR spectrum of $\text{L}^{\text{H}}$	S7
<b>Figure S3:</b> $^1\text{H}$ NMR spectrum of $\text{L}^{\text{CF}_3}$	S7
<b>Figure S4:</b> $^{13}\text{C}$ NMR spectrum of $\text{L}^{\text{CF}_3}$	S8
<b>Figure S5:</b> $^{19}\text{F}$ NMR spectrum of $\text{L}^{\text{CF}_3}$	S8
<b>Figure S6:</b> $^1\text{H}$ NMR spectrum of $\text{L}^{\text{OMe}}$	S8
<b>Figure S7:</b> $^{13}\text{C}$ NMR spectrum of $\text{L}^{\text{OMe}}$	S9
<b>Figure S8:</b> $^1\text{H}$ NMR spectrum of $\text{tpa}^{\text{OPh}}$	S9
<b>Figure S9:</b> $^{13}\text{C}$ NMR spectrum of $\text{tpa}^{\text{OPh}}$	S9
<b>Figure S10:</b> $^1\text{H}$ NMR spectrum of $\mathbf{1}^{\text{H}}$	S10
<b>Figure S11:</b> $^{13}\text{C}$ NMR spectrum of $\mathbf{1}^{\text{H}}$	S10
<b>Figure S12:</b> $^1\text{H}$ NMR spectrum of $\mathbf{1}^{\text{CF}_3}$	S10
<b>Figure S13:</b> $^{13}\text{C}$ NMR spectrum of $\mathbf{1}^{\text{CF}_3}$	S11
<b>Figure S14:</b> $^{19}\text{F}$ NMR spectrum of $\mathbf{1}^{\text{CF}_3}$	S11
<b>Figure S15:</b> $^1\text{H}$ NMR spectrum of $\mathbf{1}^{\text{OMe}}$	S11
<b>Figure S16:</b> $^{13}\text{C}$ NMR spectrum of $\mathbf{1}^{\text{OMe}}$	S12
<b>Figure S17:</b> Plot of $\mathbf{1}^{\text{R}}$ redox potential vs Hammett values	S12
<b>Figure S18:</b> Plot of $\mathbf{1}^{\text{R}}$ $^1\text{H}$ NMR NH resonance vs Hammett values	S12
<b>Figure S19:</b> IR overlay of $\text{L}^{\text{H}}$ , $\text{L}^{\text{CF}_3}$ and $\text{L}^{\text{OMe}}$	S13
<b>Figure S20:</b> IR overlay of $\mathbf{1}^{\text{H}}$ , $\mathbf{1}^{\text{CF}_3}$ and $\mathbf{1}^{\text{OMe}}$	S13
<b>Figure S21:</b> EPR spectra of $\mathbf{2}^{\text{H}}$ after room temperature decomposition	S14
<b>Figure S22:</b> UV-Vis stability study of $\mathbf{2}^{\text{H}}$	S14

<b>Figure S23:</b> Plot of $2^R$ O to Cu LMCT vs Hammett values	S15
<b>Figure S24:</b> Cyclic voltammogram of $[\text{Cu}(\text{L}^{\text{H}})]\text{BAR}'$	S15
<b>Figure S25:</b> Cyclic voltammogram of $[\text{Cu}(\text{L}^{\text{CF}_3})]\text{BAR}'$	S16
<b>Figure S26:</b> Cyclic voltammogram of $[\text{Cu}(\text{L}^{\text{OMe}})]\text{BAR}'$	S16
<b>Figure S27:</b> Overlay of square-wave voltammogram of $[\text{Cu}(\text{L}^{\text{R}})]\text{BAR}'$	S17
<b>Figure S28:</b> Cyclic and square-wave voltammogram of $[\text{Cu}(\text{tpa})]\text{BAR}'$	S17
<b>Figure S29:</b> Variable temperature $^1\text{H}$ NMR of $[\text{Cu}(\text{L}^{\text{H}})]\text{BAR}'$	S18
<b>Figure S30:</b> Variable temperature $^1\text{H}$ NMR of $[\text{Cu}(\text{tpa}^{\text{OPh}})]\text{BAR}'$	S19
Crystallography Details	S19-21
<b>Figure S31:</b> ORTEP and space-fill model of $2^{\text{H}}$	S22
References	S22

## Experimental Details

**General Considerations:** All commercially-available reagents were used as received without further purification. Tris(6-bromo-2-pyridylmethyl)amine ( $\text{Br}_3\text{tpa}$ ),<sup>1</sup>  $[\text{Cu}(\text{MeCN})_4]\text{BAR}'$  ( $\text{BAR}' = \text{B}(\text{C}_6\text{F}_5)_4$ ),<sup>2</sup> and benzyl potassium<sup>3</sup> were prepared according to the literature. All manipulations were carried out under an atmosphere of nitrogen in an Innovative Technologies Pure LabHE GP-1 glovebox or using Schlenk techniques, unless otherwise specified. NMR spectra were collected on a Varian MR400, nmrs500, or nmrs700 and were referenced to residual solvent peaks.  $^{19}\text{F}$  NMR spectra were referenced to their respective  $^1\text{H}$  spectra. Flash chromatography was performed on a Biotage Isolera One automated system using self-packed 25g or 50g columns. IR spectra were collected on a Nicolet is10 spectrometer (resolution:  $<0.4\text{ cm}^{-1}$ ) as a solution in  $\text{CH}_2\text{Cl}_2$ . EPR spectra were collected on a Bruker EMX EPR spectrometer. Electronic absorption spectra were collected on a Varian Cary-50 spectrophotometer (resolution:  $<1.5\text{ nm}$ ) using a Hellma Analytics 661.200-QX quartz probe. Voltammetry experiments were conducted using a Pine WaveNow potentiostat under  $\text{N}_2$  in a cell consisting of a glassy carbon working electrode, platinum counter electrode and a silver wire reference electrode. All voltammetry experiments were referenced to an internal ferrocene (Fc) or decamethylferrocene ( $\text{Fc}^*$ ) reference ( $\text{Fc}^* = -510\text{ mV}$  vs  $\text{Fc}/\text{Fc}^+$  in  $0.1\text{M}$   $\text{NBu}_4\text{PF}_6$  MeCN measured in-house) introduced at the end of the experiment. High-resolution mass spectrometry was collected on an Agilent 6230 TOF HPLC-MS.

**Synthesis of tris(6-phenylamino-2-pyridylmethyl)amine ( $\text{L}^{\text{H}}$ ):** In the air, a 250 mL Schlenk flask was charged with  $\text{Br}_3\text{tpa}$  (1000.0 mg; 1.897 mmol),  $\text{Pd}(\text{OAc})_2$  (38.3 mg; 0.171 mmol), BINAP (159.5 mg; 0.256 mmol),  $\text{Cs}_2\text{CO}_3$  (3709.6 mg; 11.382 mmol), and a Teflon stirbar. The flask was then subjected to multiple evacuation refill cycles with  $\text{N}_2$ . An  $\text{N}_2$ -sparged mixture of 80 mL toluene and aniline (1590.0

mg; 17.073 mmol) was added to the Schlenk flask via cannula. The solution was heated at 100°C with vigorous stirring (1200 rpm) for 12 hours. Following heating, the reaction was allowed to cool to room temperature over 1 hour. The reaction mixture was filtered over a celite plug and washed with toluene (2 x 10 mL). The combined filtrates were placed in a -20°C freezer for 8 hours over which time the product crystallized from solution. The red toluene solution was decanted and the crystals were washed with 20 mL cold toluene. The yellow crystalline solid was further purified by recrystallization from 10 mL hot acetonitrile. The off-white crystalline powder precipitates at -20°C and was isolated, washed with 5 mL cold acetonitrile, and dried overnight in vacuo to obtain pure L<sup>H</sup> (640.0 mg, 60%). IR (CH<sub>2</sub>Cl<sub>2</sub>, cm<sup>-1</sup>): 3431 and 3408 (NH). <sup>1</sup>H NMR (700 MHz, Methylene Chloride-*d*<sub>2</sub>) δ 7.49 (dd, *J* = 8.2, 7.4 Hz, 3H), 7.42 (d, *J* = 7.4 Hz, 6H), 7.30 (dd, *J* = 7.4, 7.3 Hz, 6H), 7.13 (d, *J* = 7.4 Hz, 3H), 7.00 (t, *J* = 7.3 Hz, 3H), 6.71 (d, *J* = 8.2 Hz, 3H), 6.57 (s, 3H), 3.80 (s, 6H). <sup>13</sup>C NMR (176 MHz, Methylene Chloride-*d*<sub>2</sub>) δ 159.1, 155.6, 141.4, 138.3, 129.4, 122.4, 119.8, 114.2, 107.1, 60.6. HRMS (ESI-TOF) *m/z*: [L<sup>H</sup>+H]<sup>+</sup> Calcd for C<sub>36</sub>H<sub>34</sub>N<sub>7</sub>: 564.2876; Found: 564.2879.

**Synthesis of tris(6-(4-trifluoromethylphenyl)amino-2-pyridylmethyl)amine (L<sup>CF3</sup>):**

In the air, a 20 mL glass scintillation vial was charged with Br<sub>3</sub>tpa (250.0 mg; 0.4743 mmol), Pd(OAc)<sub>2</sub> (9.6 mg; 0.0427 mmol), BINAP (39.9mg; 0.0640 mmol), Cs<sub>2</sub>CO<sub>3</sub> (927.5 mg; 2.846 mmol), 4-trifluoromethylaniline (687.8 mg; 4.2687 mmol), and a Teflon stirbar. 20 mL of N<sub>2</sub>-sparged toluene was added and the vial was quickly sealed with a Teflon-lined cap. The solution was heated at 100°C with vigorous stirring (1300 rpm) for 18 hours. Following heating, the reaction was cooled to room temperature and 20 mL of CH<sub>2</sub>Cl<sub>2</sub> was added and stirred for an additional 5 min. The slurry was filtered over a celite plug and washed with CH<sub>2</sub>Cl<sub>2</sub> (2 x 10 mL). The filtrate was then dry loaded onto silica gel via rotary evaporation. The dry loaded product was purified by flash chromatography on a Biotage Isolera One using a 25 g self-packed silica gel column. Method: 3 column volumes (CV) of 80% hexane: 20% ethyl acetate, then a gradient of 15 CV to 50% hexane: 50% ethyl acetate. Product elutes between 9-14 CV. Fractions containing product were evaporated to dryness via rotary evaporation. The light yellow solid was dried overnight in vacuo to obtain pure L<sup>CF3</sup> (275 mg; 76%). IR (CH<sub>2</sub>Cl<sub>2</sub>, cm<sup>-1</sup>): 3430 (NH). <sup>1</sup>H NMR (700 MHz, Methylene Chloride-*d*<sub>2</sub>) δ 7.64 (d, *J* = 8.4 Hz, 6H), 7.55 (dd, *J* = 8.2, 7.4 Hz, 3H), 7.51 (d, *J* = 8.4 Hz, 6H), 7.20 (d, *J* = 7.4 Hz, 3H), 6.72 (d, *J* = 8.2 Hz, 3H), 6.71 (s, 3H), 3.87 (s, 6H). <sup>13</sup>C NMR (176 MHz, Methylene Chloride-*d*<sub>2</sub>) δ 158.9, 154.5, 144.7, 138.5, 126.6 (q, *J*<sub>CF</sub> = 4 Hz), 125.1 (q, *J*<sub>CF</sub> = 271 Hz), 122.9 (q, *J*<sub>CF</sub> = 32 Hz), 118.0, 115.4, 108.8, 60.6. <sup>19</sup>F NMR (377 MHz, Methylene Chloride-*d*<sub>2</sub>) δ -61.9. HRMS (ESI-TOF) *m/z*: [L<sup>CF3</sup>+H]<sup>+</sup> Calcd for C<sub>39</sub>H<sub>31</sub>F<sub>9</sub>N<sub>7</sub>: 768.2497; Found: 768.2493.

**Synthesis of tris(6-(4-methoxyphenyl)amino-2-pyridylmethyl)amine (L<sup>OMe</sup>):**

In the air, a 20 mL glass scintillation vial was charged with Br<sub>3</sub>tpa (250.0 mg; 0.4743 mmol), Pd(OAc)<sub>2</sub> (9.6 mg; 0.0427 mmol), BINAP (39.9mg; 0.0640 mmol), Cs<sub>2</sub>CO<sub>3</sub> (927.5 mg; 2.846 mmol), 4-methoxyaniline (525.7 mg; 4.2687 mmol), and a Teflon stirbar. 20 mL of N<sub>2</sub>-sparged toluene was added and the vial was quickly sealed with a Teflon-lined cap. The solution was heated at 100°C with vigorous stirring (1300

rpm) for 18 hours. Following heating, the reaction was cooled to room temperature and 20 mL of CH<sub>2</sub>Cl<sub>2</sub> was added and stirred for an additional 5 min. The slurry was filtered over a celite plug and washed with CH<sub>2</sub>Cl<sub>2</sub> (2 x 10 mL). The filtrate was then dry loaded onto silica gel via rotary evaporation. The dry loaded product was purified by flash chromatography on a Biotage Isolera One using a 25 g self-packed silica gel column. Method: 3 column volumes (CV) of 60% hexane: 40% ethyl acetate, then a gradient of 20 CV to 100% ethyl acetate. Product elutes between 13-18 CV. Fractions containing product were evaporated to dryness via rotary evaporation. The brown solid was further purified by recrystallization from 4 mL hot toluene. The light brown powder precipitates at room temperature and was isolated and dried overnight in vacuo to obtain pure L<sup>OMe</sup> (228 mg, 74%). IR (CH<sub>2</sub>Cl<sub>2</sub>, cm<sup>-1</sup>): 3433 and 3409 (NH). <sup>1</sup>H NMR (700 MHz, Methylene Chloride-*d*<sub>2</sub>) δ 7.44 (dd, *J* = 8.2, 7.4 Hz, 3H), 7.30 (d, *J* = 8.8 Hz, 6H), 7.05 (d, *J* = 7.4 Hz, 3H), 6.87 (d, *J* = 8.8 Hz, 6H), 6.55 (d, *J* = 8.2 Hz, 3H), 6.41 (s, 3H), 3.78 (s, 9H), 3.74 (s, 6H). <sup>13</sup>C NMR (176 MHz, Methylene Chloride-*d*<sub>2</sub>) δ 159.1, 156.7, 156.2, 138.2, 134.2, 123.3, 114.7, 113.5, 105.9, 60.6, 55.9. HRMS (ESI-TOF) *m/z*: [L<sup>OMe</sup>+H]<sup>+</sup> Calcd for C<sub>39</sub>H<sub>40</sub>N<sub>7</sub>O<sub>3</sub>: 654.3193; Found: 654.3188.

**Synthesis of tris(6-phenoxy-2-pyridylmethyl)amine (tpa<sup>OPh</sup>):** To a freshly prepared 3 mL solution of benzyl potassium (173.0 mg; 1.328 mmol) in THF was added a 3 mL solution of phenol (142.8 mg; 1.518 mmol) in THF. The mixture was let stir for 1 min as KOPh precipitated as a white solid. The THF was then removed in vacuo. To the vial containing KOPh was added CuI (36.1 mg; 0.190 mmol), Br<sub>3</sub>tpa (200.0 mg; 0.3795 mmol) and 10 mL toluene. The mixture was stirred at 100°C for 20 hours followed by cooling to room temperature. 20 mL of CH<sub>2</sub>Cl<sub>2</sub> was added and stirred for an additional 5 min. The slurry was filtered over a celite plug and washed with CH<sub>2</sub>Cl<sub>2</sub> (2 x 10 mL). The filtrate was then dry loaded onto silica gel via rotary evaporation. The dry loaded product was purified by flash chromatography on a Biotage Isolera One using a 25 g self-packed silica gel column. Method: 3 column volumes (CV) of 95% hexane: 5% ethyl acetate, then a gradient of 15 CV to 100% ethyl acetate. Product elutes between 8-9 CV. Fractions containing product were evaporated to dryness via rotary evaporation. The product was further purified by recrystallization from 4 mL hot ethanol and dried overnight in vacuo to yield pure tpa<sup>OPh</sup> (81.1 mg, 38%) as a white solid. <sup>1</sup>H NMR (700 MHz, Methylene Chloride-*d*<sub>2</sub>) δ 7.56 (dd, *J* = 8.1, 7.4 Hz, 3H), 7.37 (dd, *J* = 7.7, 7.4 Hz, 6H), 7.18 (t, *J* = 7.4 Hz, 3H), 7.15 (d, *J* = 7.4 Hz, 3H), 7.11 (d, *J* = 7.7 Hz, 6H), 6.72 (d, *J* = 8.1 Hz, 3H), 3.60 (s, 6H). <sup>13</sup>C NMR (176 MHz, Methylene Chloride-*d*<sub>2</sub>) δ 163.4, 158.6, 155.0, 140.1, 129.9, 124.6, 121.5, 118.0, 109.8, 59.4. HRMS (ESI-TOF) *m/z*: [tpa<sup>OPh</sup>+H]<sup>+</sup> Calcd for C<sub>36</sub>H<sub>31</sub>N<sub>4</sub>O<sub>3</sub>: 567.2396; Found: 567.2465.

**Synthesis of Cu(L<sup>H</sup>)Cl (1<sup>H</sup>):** CuCl (5.9 mg; 0.0596 mmol), L<sup>H</sup> (35.3 mg ; 0.0626 mmol), 3 mL THF, and a Teflon stir bar were added to a 20 mL glass scintillation vial and stirred for 48 hours at room temperature. The yellow solution was then evaporated to dryness with vacuum. The yellow solid was dissolved in 2 mL CH<sub>2</sub>Cl<sub>2</sub>, filtered through a glass pipette fitted with glass filter paper, and concentrated to 1 mL CH<sub>2</sub>Cl<sub>2</sub>. The product was then precipitated by addition of 5 mL diethyl ether. The

yellow powder was collected and washed twice with 3 mL diethyl ether and dried overnight under vacuum to obtain pure **1<sup>H</sup>** (24.6 mg, 59%). A crystal suitable for X-ray diffraction was grown by layering pentane over a concentrated toluene solution at -30°C. IR (CH<sub>2</sub>Cl<sub>2</sub>, cm<sup>-1</sup>): 3223 (NH). <sup>1</sup>H NMR (700 MHz, Methylene Chloride-*d*<sub>2</sub>) δ 9.89 (s, 3H), 7.43 (dd, *J* = 8.4, 7.2 Hz, 3H), 7.32 (m, 12H), 7.03 (t, *J* = 7.1 Hz, 3H), 7.01 (d, *J* = 8.4 Hz, 3H), 6.59 (d, *J* = 7.2 Hz, 3H), 3.69 (s, 6H). <sup>13</sup>C NMR (176 MHz, Methylene Chloride-*d*<sub>2</sub>) δ 157.3, 155.3, 140.9, 138.6, 129.6, 123.3, 121.2, 113.8, 107.1, 59.3. HRMS (ESI-TOF) *m/z*: [Cu(L<sup>H</sup>)Cl]<sup>+</sup> Calcd for C<sub>36</sub>H<sub>33</sub>ClCuN<sub>7</sub>: 661.1782; Found: 661.1763. Anal. calcd for C<sub>36</sub>H<sub>33</sub>ClCuN<sub>7</sub>: C, 65.25; H, 5.02; N, 14.80. Found: C, 64.96; H, 5.11; N, 14.62.

**Synthesis of Cu(L<sup>CF3</sup>)Cl (**1<sup>CF3</sup>**):** CuCl (1.5 mg; 0.0152 mmol), L<sup>CF3</sup> (11.6 mg ; 0.0152 mmol), 3 mL benzene, and a Teflon stir bar were added to a 20 mL glass scintillation vial and stirred for 24 hours at room temperature. A yellow precipitate formed in solution that was then isolated by filtration over a glass pipette fitted with a glass filter plug. The yellow solid was washed twice with benzene (2 mL) and twice with pentane (2 mL) before dissolving in 5 mL CH<sub>2</sub>Cl<sub>2</sub> and passing over the frit. The light yellow solution was pumped down to dryness in vacuo overnight to yield pure **1<sup>CF3</sup>** (9.7 mg, 74%). IR (CH<sub>2</sub>Cl<sub>2</sub>, cm<sup>-1</sup>): 3221 (NH). <sup>1</sup>H NMR (700 MHz, Methylene Chloride-*d*<sub>2</sub>) δ 10.17 (s, 3H), 7.54 (d, *J* = 8.3 Hz, 6H), 7.52 (dd, *J* = 8.3, 7.3 Hz, 3H), 7.42 (d, *J* = 8.3 Hz, 6H), 7.12 (d, *J* = 8.3 Hz, 3H), 6.69 (d, *J* = 7.3 Hz, 3H), 3.73 (s, 6H). <sup>13</sup>C NMR (176 MHz, Methylene Chloride-*d*<sub>2</sub>) δ 156.0, 155.5, 144.4, 139.0, 126.8, 126.5 (q, *J*<sub>CF</sub> = 271 Hz), 124.1 (q, *J*<sub>CF</sub> = 31 Hz), 119.2, 115.1, 108.2, 59.3. (Note: **1<sup>CF3</sup>** is only slightly soluble in CH<sub>2</sub>Cl<sub>2</sub> leading to a weak <sup>13</sup>C NMR signal). <sup>19</sup>F NMR (377 MHz, Methylene Chloride-*d*<sub>2</sub>) δ -62.1. HRMS (ESI-TOF) *m/z*: [Cu(L<sup>CF3</sup>)Cl]<sup>+</sup> Calcd for C<sub>39</sub>H<sub>30</sub>ClCuF<sub>9</sub>N<sub>7</sub>: 865.1404; Found: 865.1378. Anal. calcd for C<sub>39</sub>H<sub>30</sub>ClCuF<sub>9</sub>N<sub>7</sub>: C, 54.05; H, 3.49; N, 11.31. Found: C, 54.14; H, 3.44; N, 11.19.

**Synthesis of Cu(L<sup>OMe</sup>)Cl (**1<sup>OMe</sup>**):** CuCl (2.8 mg; 0.0283 mmol), L<sup>OMe</sup> (19.4 mg ; 0.0297 mmol), 3 mL THF, and a Teflon stir bar were added to a 20 mL glass scintillation vial and stirred for 48 hours at room temperature. The yellow solution was then evaporated to dryness with vacuum. The yellow solid was dissolved in 2 mL CH<sub>2</sub>Cl<sub>2</sub>, filtered through a glass pipette fitted with glass filter paper, and concentrated to 1 mL CH<sub>2</sub>Cl<sub>2</sub>. 5 mL diethyl ether was added to the vial and the product slowly crystallized out of solution as yellow needles over 1 hour. The yellow crystals were washed twice with 3 mL diethyl ether and dried overnight under vacuum to obtain pure **1<sup>OMe</sup>** (19.3 mg, 86%). IR (CH<sub>2</sub>Cl<sub>2</sub>, cm<sup>-1</sup>): 3220 (NH). <sup>1</sup>H NMR (700 MHz, Methylene Chloride-*d*<sub>2</sub>) δ 9.72 (s, 3H), 7.37 (dd, *J* = 8.1, 7.7 Hz, 3H), 7.286 (d, *J* = 8.4 Hz, 6H), 6.88 (d, *J* = 8.4 Hz, 6H), 6.79 (d, *J* = 8.1 Hz, 3H), 6.53 (d, *J* = 7.7 Hz, 3H), 3.78 (s, 9H), 3.65 (s, 6H). <sup>13</sup>C NMR (176 MHz, Methylene Chloride-*d*<sub>2</sub>) δ 158.4, 156.6, 155.2, 138.4, 133.7, 124.2, 114.9, 113.0, 106.4, 59.2, 55.8. HRMS (ESI-TOF) *m/z*: [Cu(L<sup>OMe</sup>)Cl]<sup>+</sup> Calcd for C<sub>39</sub>H<sub>39</sub>ClCuN<sub>7</sub>O<sub>3</sub>: 751.2099; Found: 751.2082. Anal. calcd for C<sub>39</sub>H<sub>39</sub>ClCuN<sub>7</sub>O<sub>3</sub>: C, 62.23; H, 5.22; N, 13.02. Found: C, 61.79; H, 5.10; N, 12.76.

**Synthesis of [(Cu(L<sup>H</sup>))<sub>2</sub>(O<sub>2</sub>)] [BAR']<sub>2</sub> (**2<sup>H</sup>**):** In a nitrogen-filled glovebox, [Cu(MeCN)<sub>4</sub>]BAR' (6.9 mg; 0.0076 mmol) and L<sup>H</sup> (4.3 mg; 0.0076 mmol) were

dissolved in 5.1 mL CH<sub>2</sub>Cl<sub>2</sub> in a 25 mL round bottom flask to produce a 1.5 mM solution of [Cu(L<sup>H</sup>)]BAR'. The round bottom flask was sealed with a rubber septum and cable tie, removed from the glovebox, and transferred via cannula to a dry, N<sub>2</sub>-filled vessel containing the UV-Vis dip probe. The dip probe glassware containing [Cu(L<sup>H</sup>)]BAR' was placed in a -70°C dry ice/acetone bath and the solution stirred for ~5 min. Dry oxygen was bubbled through the solution while the headspace was allowed to purge resulting in a color change from colorless to brown indicating formation of **2<sup>H</sup>**. Completion of the reaction was assessed by UV-Vis. [Note: due to the insolubility of **2<sup>CF3</sup>** in pure CH<sub>2</sub>Cl<sub>2</sub>, comparison spectra were taken in 1:1 CH<sub>2</sub>Cl<sub>2</sub>:acetone by first formation of **2<sup>H</sup>** in 3 mM [Cu(L<sup>H</sup>)]BAR' CH<sub>2</sub>Cl<sub>2</sub> followed by slow addition of cold acetone.] A crystal of **2<sup>H</sup>** suitable for X-ray diffraction was obtained by allowing a concentrated CH<sub>2</sub>Cl<sub>2</sub> solution of [Cu(L<sup>H</sup>)]BAR' to sit under an atmosphere of dry O<sub>2</sub> in a sealed Schlenk flask for 3 days in a -80°C freezer.  $\lambda_{\text{max}}$  (1:1, CH<sub>2</sub>Cl<sub>2</sub>:acetone)/nm 457 ( $\epsilon$ , M<sup>-1</sup>cm<sup>-1</sup> 3100), 701 (600), 830 (600).

**Synthesis of [(Cu(L<sup>CF3</sup>))<sub>2</sub>(O<sub>2</sub>)]BAR'<sub>2</sub> (**2<sup>CF3</sup>**):** In a nitrogen-filled glovebox, [Cu(MeCN)<sub>4</sub>]BAR' (8.2 mg; 0.0090 mmol) and L<sup>CF3</sup> (6.9 mg; 0.0090 mmol) were dissolved in 3.0 mL CH<sub>2</sub>Cl<sub>2</sub> in a 25 mL round bottom flask to produce a 3.0 mM solution of [Cu(L<sup>CF3</sup>)]BAR'. The round bottom flask was sealed with a rubber septum and cable tie, removed from the glovebox, and transferred via cannula to a dry, N<sub>2</sub>-filled vessel containing the UV-Vis dip probe. The dip probe glassware containing [Cu(L<sup>CF3</sup>)]BAR' was placed in a -70°C dry ice/acetone bath and the solution stirred for ~5 min. Dry oxygen was bubbled through the solution while the headspace was allowed to purge resulting in a color change from colorless to brown followed by immediate formation of a light brown precipitate. The solid (**2<sup>CF3</sup>**) could be dissolved by addition of 1 part cold acetone to the solution in order to extract UV-Vis data. Completion of the reaction was assessed by UV-Vis.  $\lambda_{\text{max}}$  (1:1, CH<sub>2</sub>Cl<sub>2</sub>:acetone)/nm 450 ( $\epsilon$ , M<sup>-1</sup>cm<sup>-1</sup> 2400), 696 (600), 831 (600).

**Synthesis of [(Cu(L<sup>OMe</sup>))<sub>2</sub>(O<sub>2</sub>)]BAR'<sub>2</sub> (**2<sup>OMe</sup>**):** In a nitrogen-filled glovebox, [Cu(MeCN)<sub>4</sub>]BAR' (6.1 mg; 0.0067 mmol) and L<sup>OMe</sup> (4.4 mg; 0.0067 mmol) were dissolved in 4.5 mL CH<sub>2</sub>Cl<sub>2</sub> in a 25 mL round bottom flask to produce a 1.5 mM solution of [Cu(L<sup>OMe</sup>)]BAR'. The round bottom flask was sealed with a rubber septum and cable tie, removed from the glovebox, and transferred via cannula to a dry, N<sub>2</sub>-filled vessel containing the UV-Vis dip probe. The dip probe glassware containing [Cu(L<sup>OMe</sup>)]BAR' was placed in a -70°C dry ice/acetone bath and the solution stirred for ~5 min. Dry oxygen was bubbled through the solution while the headspace was allowed to purge resulting in a color change from colorless to brown indicating formation of **2<sup>OMe</sup>**. Completion of the reaction was assessed by UV-Vis. [Note: due to the insolubility of **2<sup>CF3</sup>** in pure CH<sub>2</sub>Cl<sub>2</sub>, comparison spectra were taken in 1:1 CH<sub>2</sub>Cl<sub>2</sub>:acetone by first formation of **2<sup>OMe</sup>** in 3 mM [Cu(L<sup>OMe</sup>)]BAR' CH<sub>2</sub>Cl<sub>2</sub> followed by slow addition of cold acetone.]  $\lambda_{\text{max}}$  (1:1, CH<sub>2</sub>Cl<sub>2</sub>:acetone)/nm 460 ( $\epsilon$ , M<sup>-1</sup>cm<sup>-1</sup> 2500), 696 (500), 827 (500).

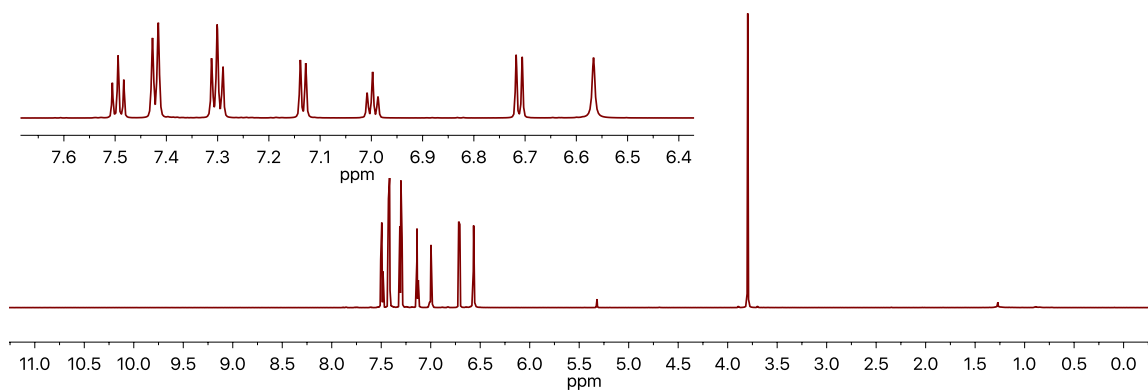


**Figure S1:** 700 MHz  $^1\text{H}$  NMR spectrum of  $\text{L}^{\text{H}}$  collected at 25°C in  $\text{CD}_2\text{Cl}_2$ .

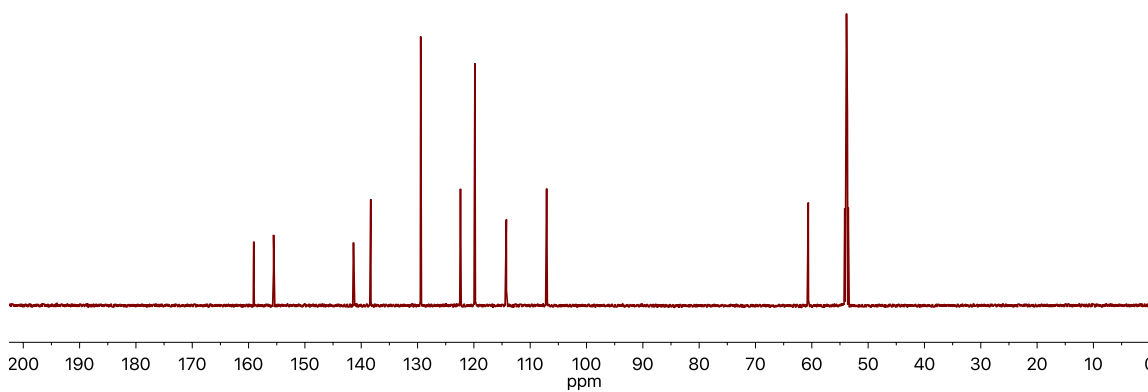


**Figure S2:** 176 MHz  $^{13}\text{C}$  NMR spectrum of  $\text{L}^{\text{H}}$  collected at 25°C in  $\text{CD}_2\text{Cl}_2$ .

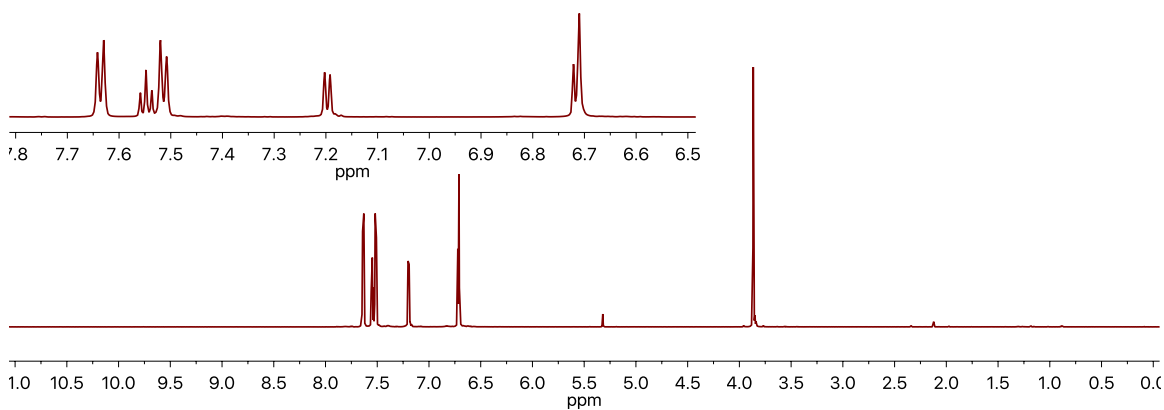


**Figure S3:** 700 MHz  $^1\text{H}$  NMR spectrum of  $\text{L}^{\text{CF}_3}$  collected at 25°C in  $\text{CD}_2\text{Cl}_2$ .

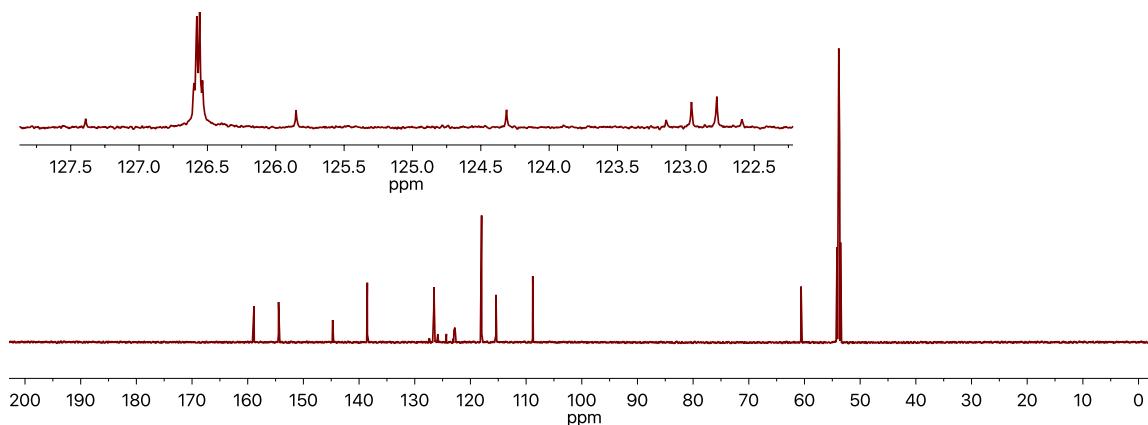


**Figure S4:** 176 MHz  $^{13}\text{C}$  NMR spectrum of  $\text{L}^{\text{CF}_3}$  collected at 25°C in  $\text{CD}_2\text{Cl}_2$ .

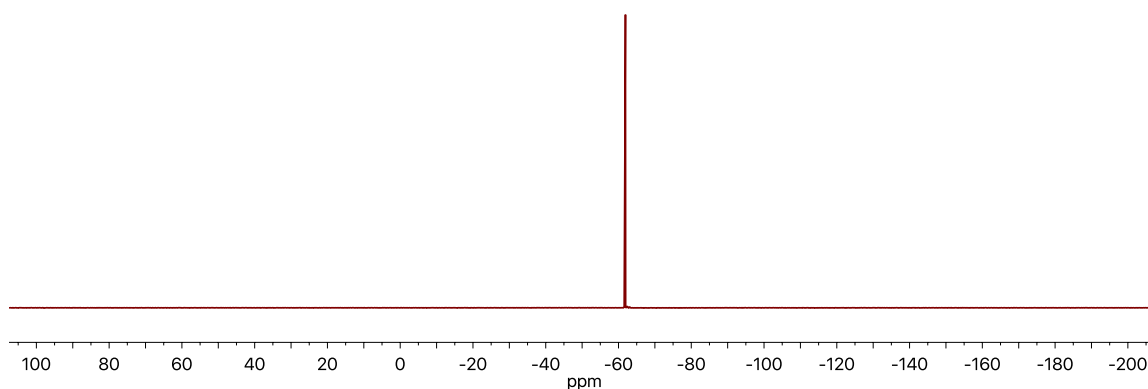


**Figure S5:** 377 MHz  $^{19}\text{F}$  NMR spectrum of  $\text{L}^{\text{CF}_3}$  collected at 25°C in  $\text{CD}_2\text{Cl}_2$ .

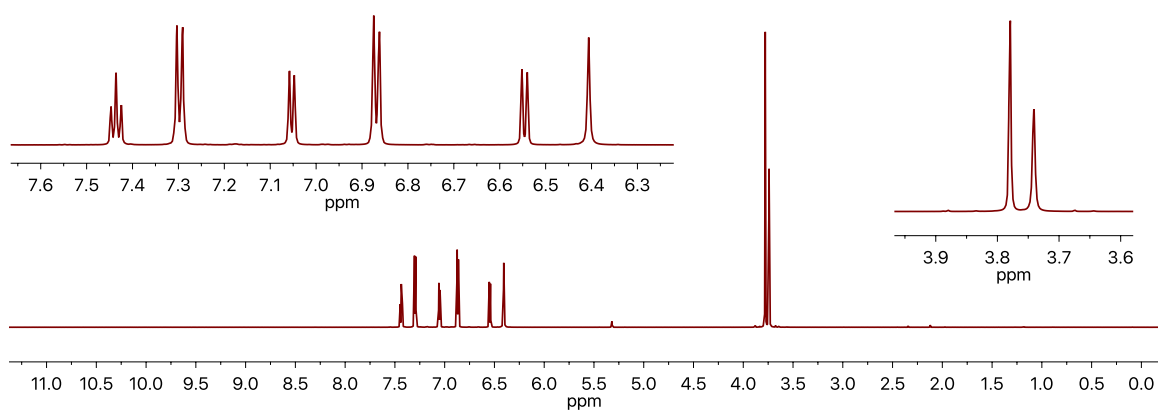


**Figure S6:** 700 MHz  $^1\text{H}$  NMR spectrum of  $\text{L}^{\text{OMe}}$  collected at 25°C in  $\text{CD}_2\text{Cl}_2$ .



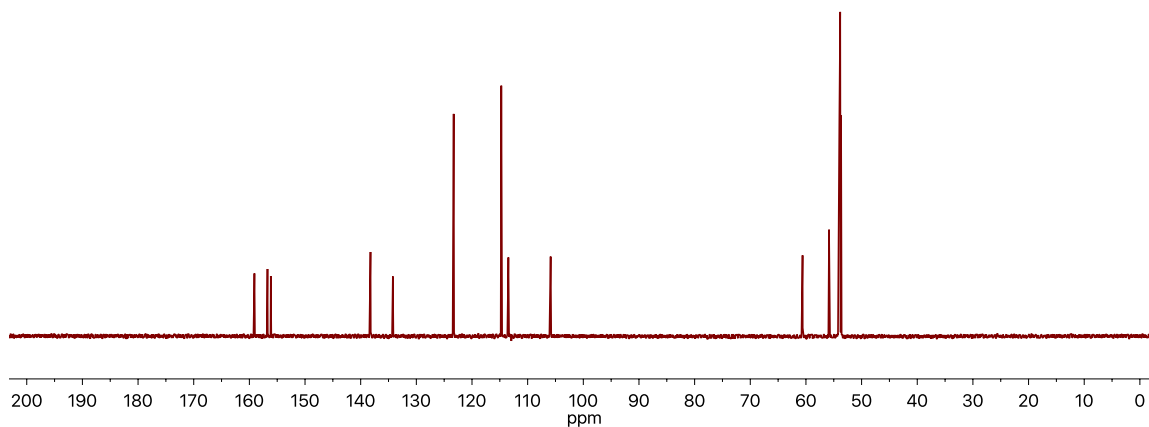


**Figure S7:** 176 MHz  $^{13}\text{C}$  NMR spectrum of  $\text{L}^{\text{OMe}}$  collected at 25°C in  $\text{CD}_2\text{Cl}_2$ .

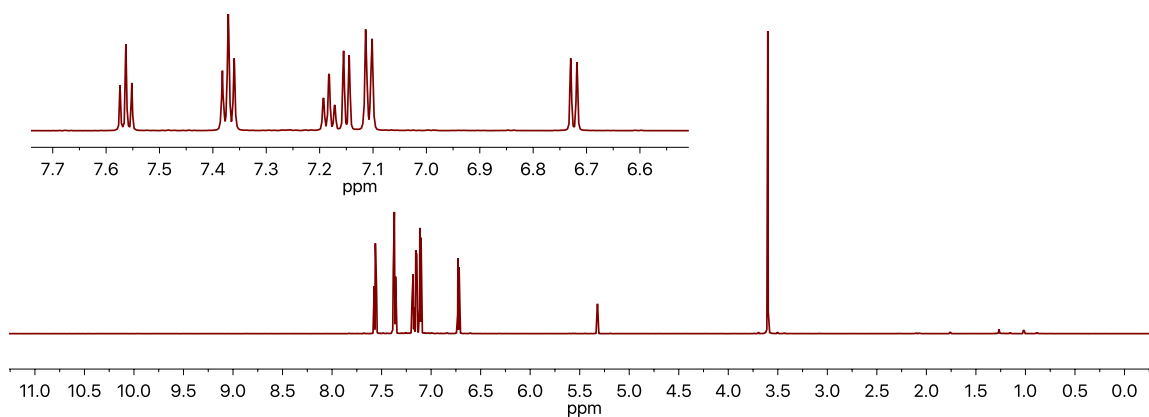


**Figure S8:** 700 MHz  $^1\text{H}$  NMR spectrum of  $\text{tpa}^{\text{OPh}}$  collected at 25°C in  $\text{CD}_2\text{Cl}_2$ .

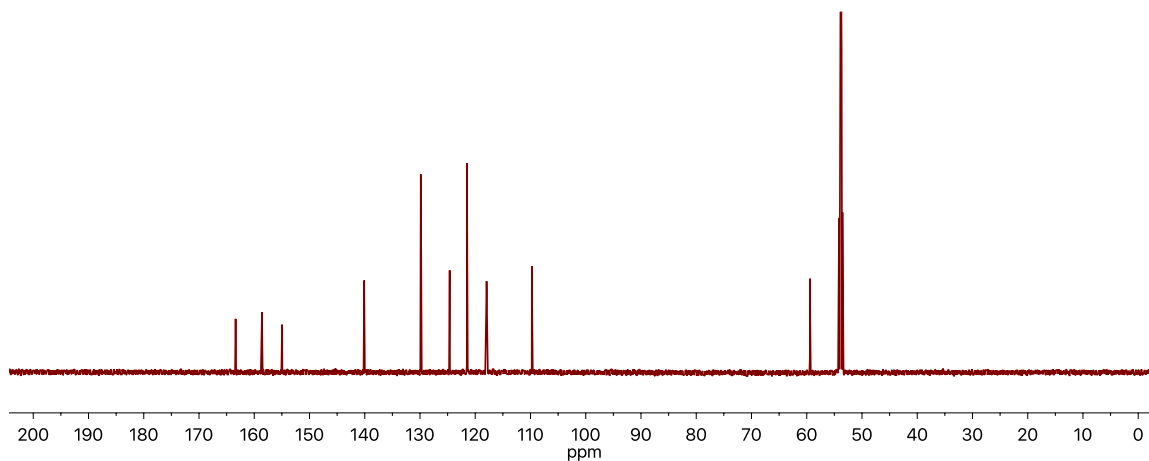


**Figure S9:** 176 MHz  $^{13}\text{C}$  NMR spectrum of  $\text{tpa}^{\text{OPh}}$  collected at 25°C in  $\text{CD}_2\text{Cl}_2$ .

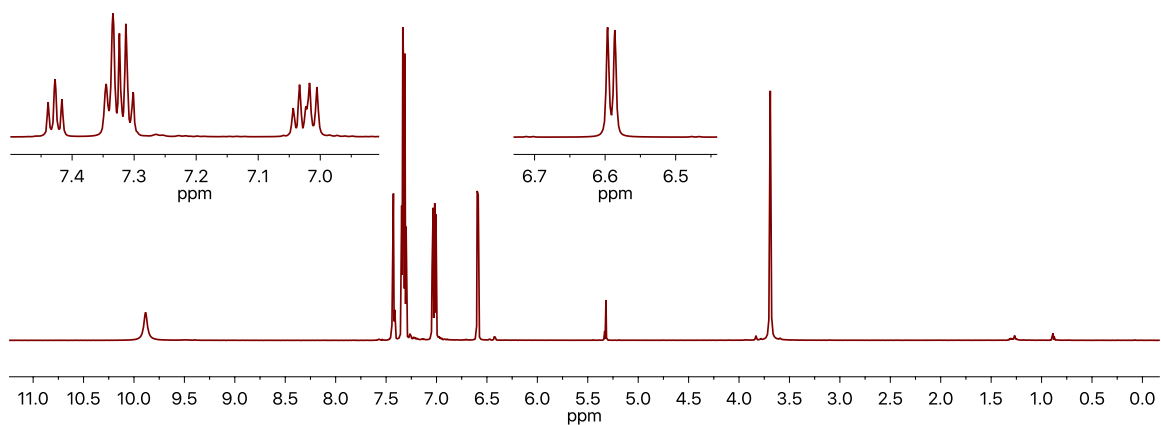


**Figure S10:** 700 MHz  $^1\text{H}$  NMR spectrum of  $1^{\text{H}}$  collected at 25°C in  $\text{CD}_2\text{Cl}_2$ .

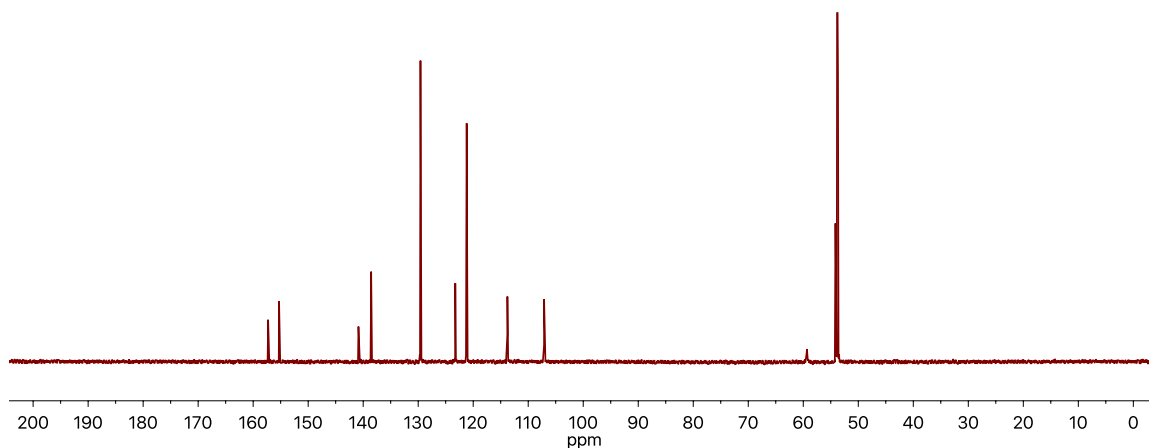


**Figure S11:** 176 MHz  $^{13}\text{C}$  NMR spectrum of  $1^{\text{H}}$  collected at 25°C in  $\text{CD}_2\text{Cl}_2$ .

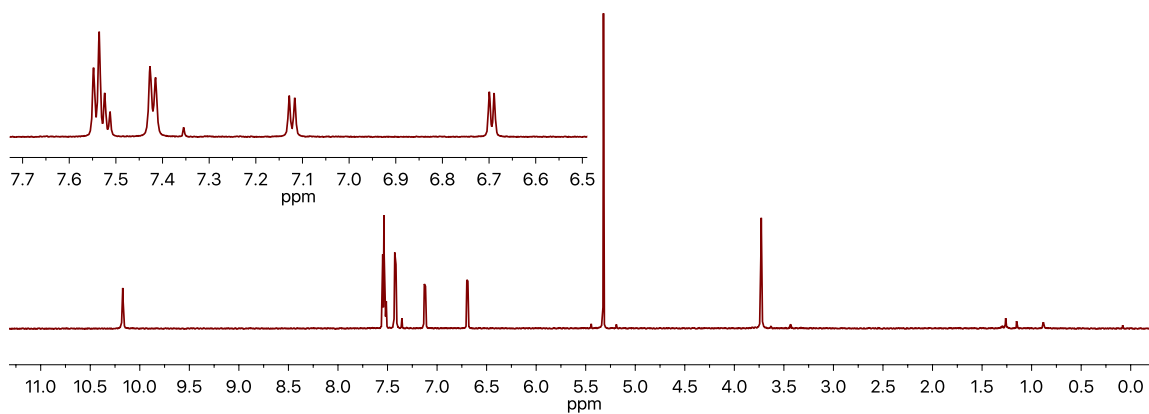


**Figure S12:** 700 MHz  $^1\text{H}$  NMR spectrum of  $1^{\text{CF}_3}$  collected at 25°C in  $\text{CD}_2\text{Cl}_2$ .

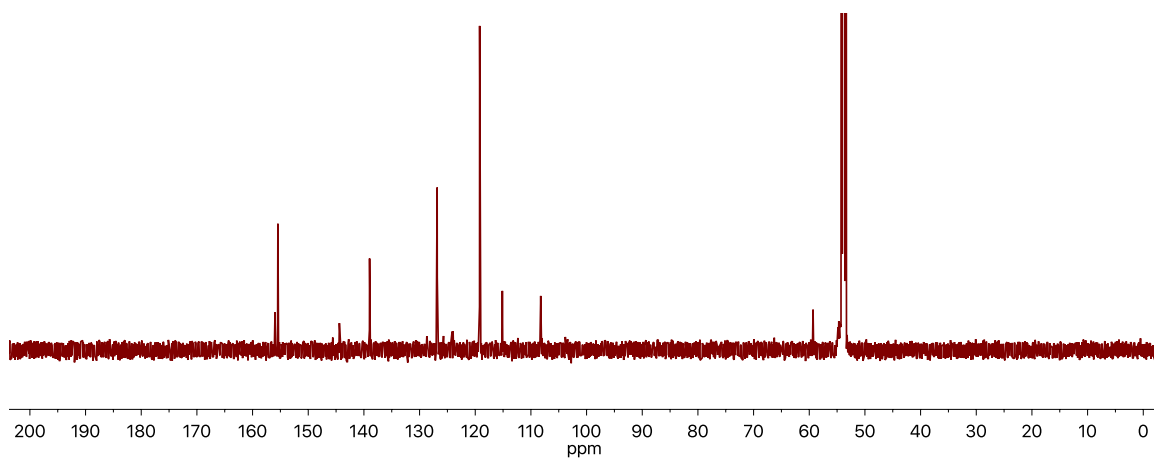


**Figure S13:** 176 MHz  $^{13}\text{C}$  NMR spectrum of  $\mathbf{1}^{\text{CF}_3}$  collected at 25°C in  $\text{CD}_2\text{Cl}_2$ .

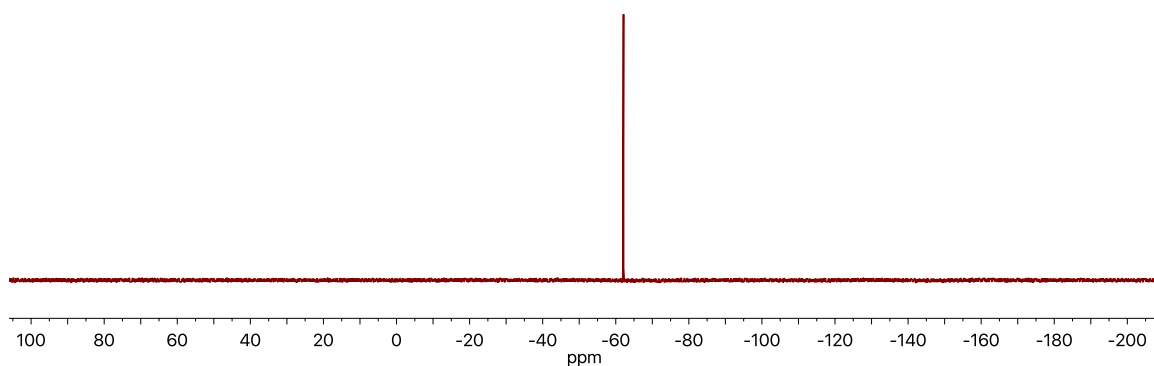


**Figure S14:** 377 MHz  $^{19}\text{F}$  NMR spectrum of  $\mathbf{1}^{\text{CF}_3}$  collected at 25°C in  $\text{CD}_2\text{Cl}_2$ .

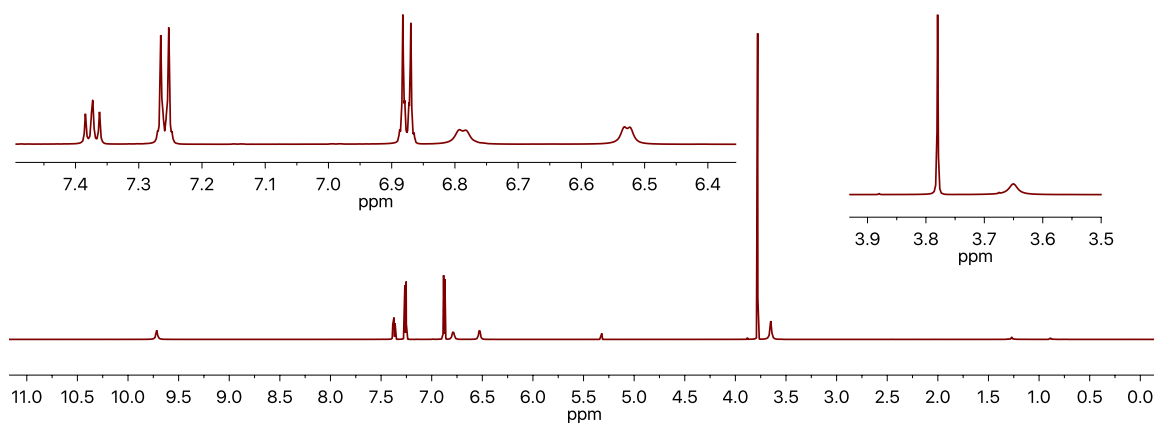


**Figure S15:** 700 MHz  $^1\text{H}$  NMR spectrum of  $\mathbf{1}^{\text{OMe}}$  collected at 25°C in  $\text{CD}_2\text{Cl}_2$ .

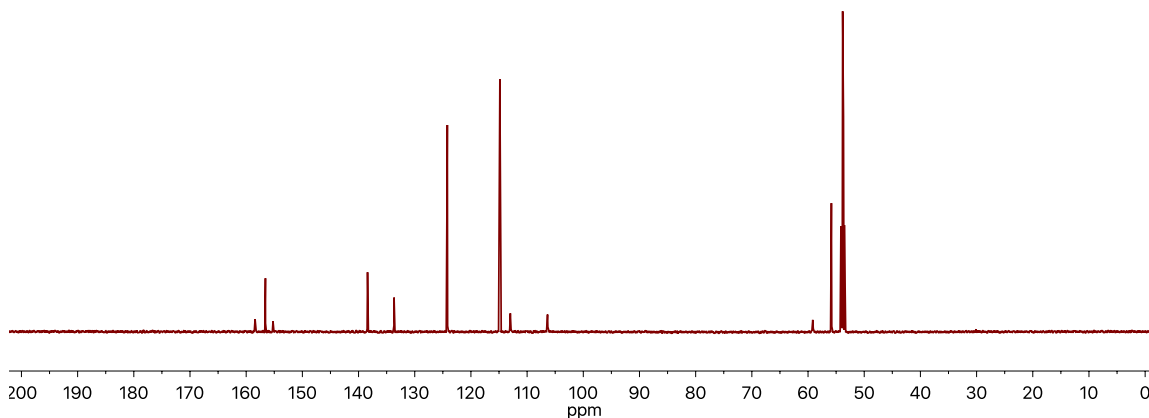


**Figure S16:** 176 MHz  $^{13}\text{C}$  NMR spectrum of **1**<sup>OMe</sup> collected at 25°C in  $\text{CD}_2\text{Cl}_2$ .

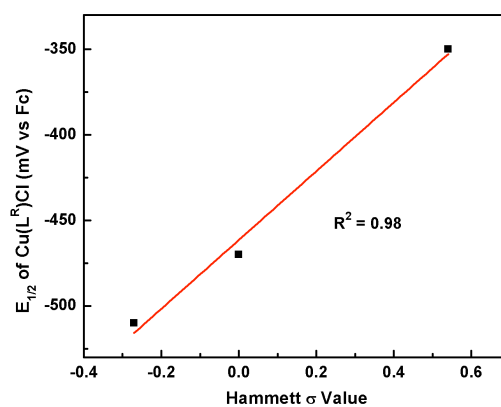


**Figure S17:** Plot of the  $E_{1/2}$  of **1**<sup>CF<sub>3</sub></sup>, **1**<sup>H</sup>, and **1**<sup>OMe</sup> in  $\text{CH}_2\text{Cl}_2$  compared to the Hammett values of *p*-CF<sub>3</sub>, *p*-H, and *p*-OMe.

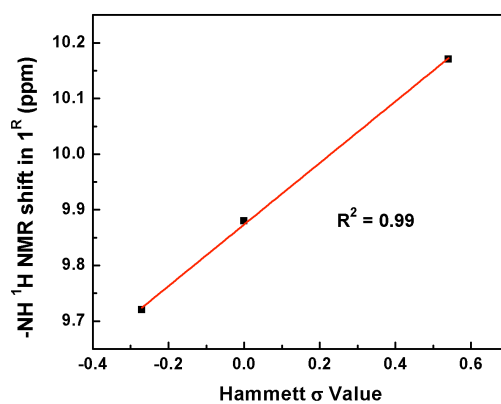


**Figure S18:** Plot of the NH peak of **1**<sup>CF<sub>3</sub></sup>, **1**<sup>H</sup>, and **1**<sup>OMe</sup> in  $\text{CD}_2\text{Cl}_2$  by  $^1\text{H}$  NMR (700 MHz) compared to the Hammett values of *p*-CF<sub>3</sub>, *p*-H, and *p*-OMe.

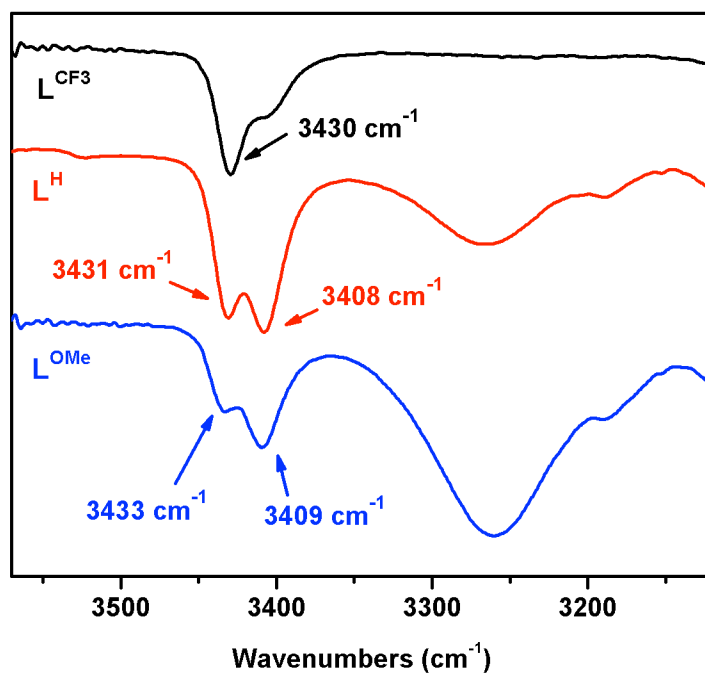


**Figure S19:** Infrared spectrum overlay of  $L^{CF_3}$ ,  $L^H$ , and  $L^{OMe}$  in  $CH_2Cl_2$ .

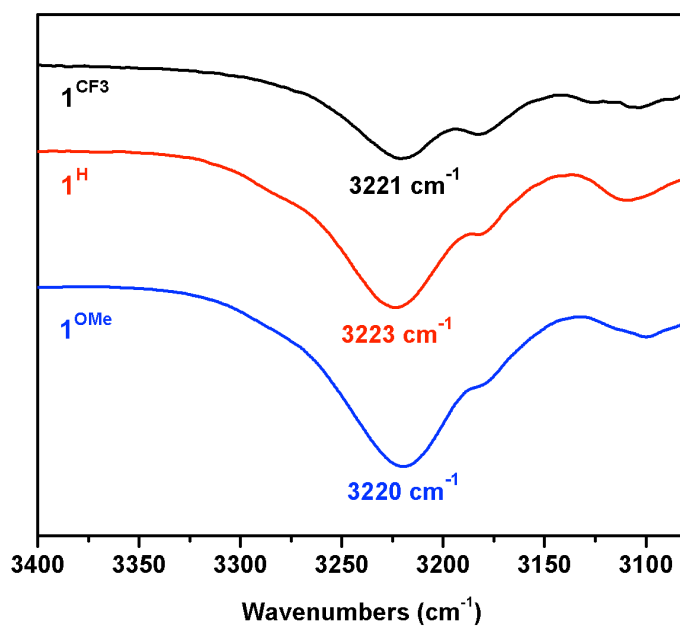


**Figure S20:** Infrared spectrum overlay of  $1^{CF_3}$ ,  $1^H$ , and  $1^{OMe}$  in  $CH_2Cl_2$ .

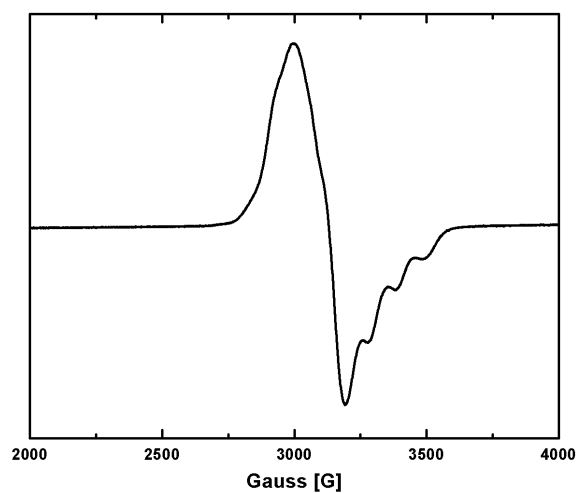


**Figure S21:** EPR spectra of  $2^{\text{H}}$  in  $\text{CH}_2\text{Cl}_2$  (120 K) taken with a solution kept at  $-70^\circ\text{C}$  (black) and then warmed to  $25^\circ\text{C}$  for 10 min (red). Some decomposition of  $2^{\text{H}}$  is evident in the initial spectrum.

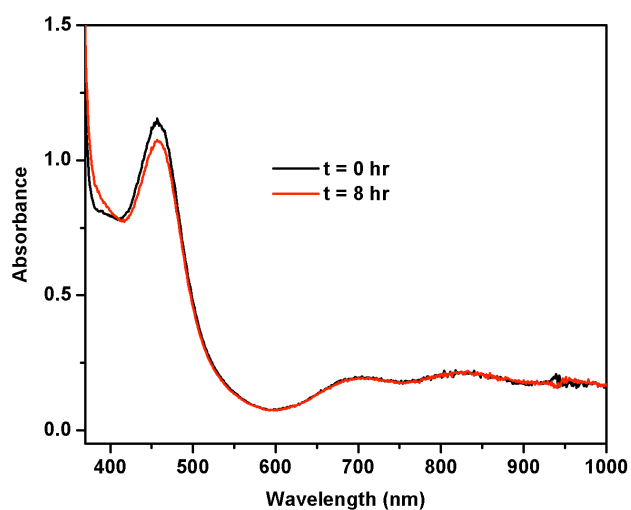


**Figure S22:** UV-Vis spectra of  $2^{\text{H}}$  in  $\text{CH}_2\text{Cl}_2$  (0.75 mM) in a  $-70^\circ\text{C}$  (acetone/ $\text{CO}_2$ ) bath immediately after adding  $\text{O}_2$  and after 8 hours.

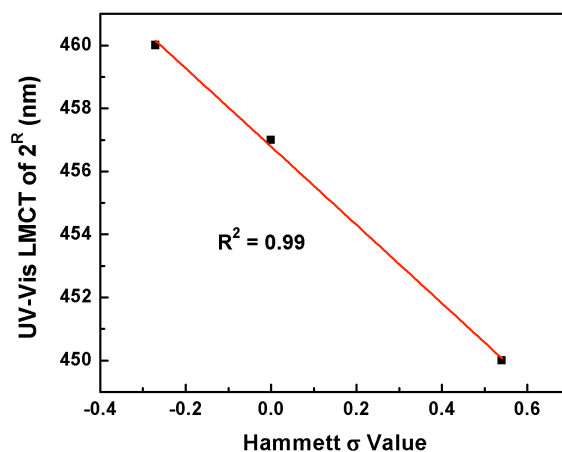


**Figure S23:** Plot of the O to Cu LMCT band in  $2^{CF_3}$ ,  $2^H$ , and  $2^{OMe}$  in 1:1  $CH_2Cl_2$ :acetone determined by UV-Vis compared to the Hammett values of  $p$ - $CF_3$ ,  $p$ -H, and  $p$ -OMe.

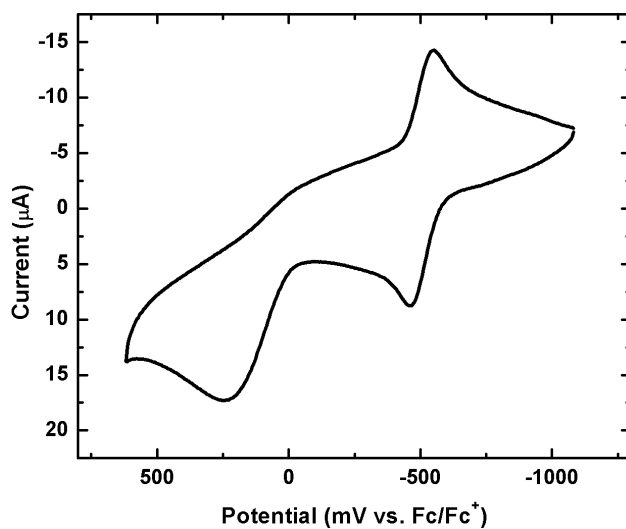


**Figure S24:** Cyclic voltammogram of  $[Cu(L^H)]BAR'$  in 0.1M  $NBu_4PF_6$  MeCN with  $Fc^*$  as internal reference ( $Fc^*/Fc^{*+} = -510$  mV vs  $Fc/Fc^+$ )

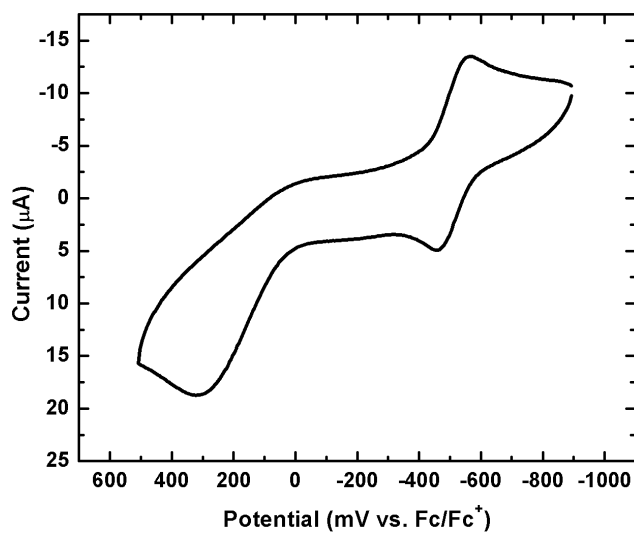


**Figure S25:** Cyclic voltammogram of  $[\text{Cu}(\text{L}^{\text{CF}_3})]\text{BAR}'$  in 0.1M  $\text{NBu}_4\text{PF}_6$  MeCN with  $\text{Fc}^*$  as internal reference ( $\text{Fc}^*/\text{Fc}^{*+} = -510$  mV vs  $\text{Fc}/\text{Fc}^+$ )

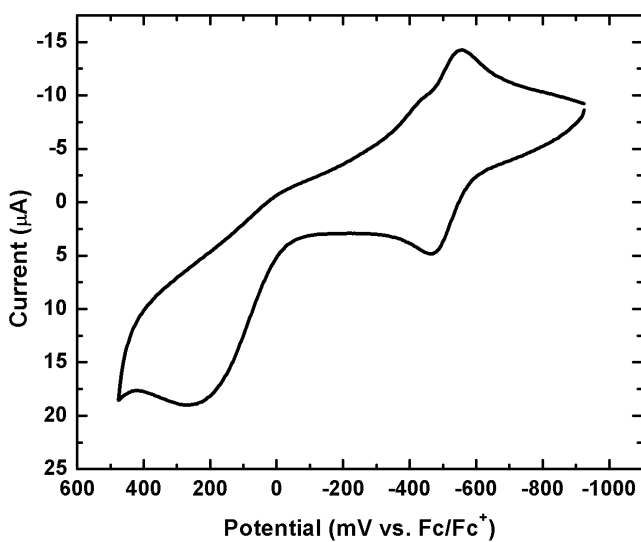


**Figure S26:** Cyclic voltammogram of  $[\text{Cu}(\text{L}^{\text{OMe}})]\text{BAR}'$  in 0.1M  $\text{NBu}_4\text{PF}_6$  MeCN with  $\text{Fc}^*$  as internal reference ( $\text{Fc}^*/\text{Fc}^{*+} = -510$  mV vs  $\text{Fc}/\text{Fc}^+$ )



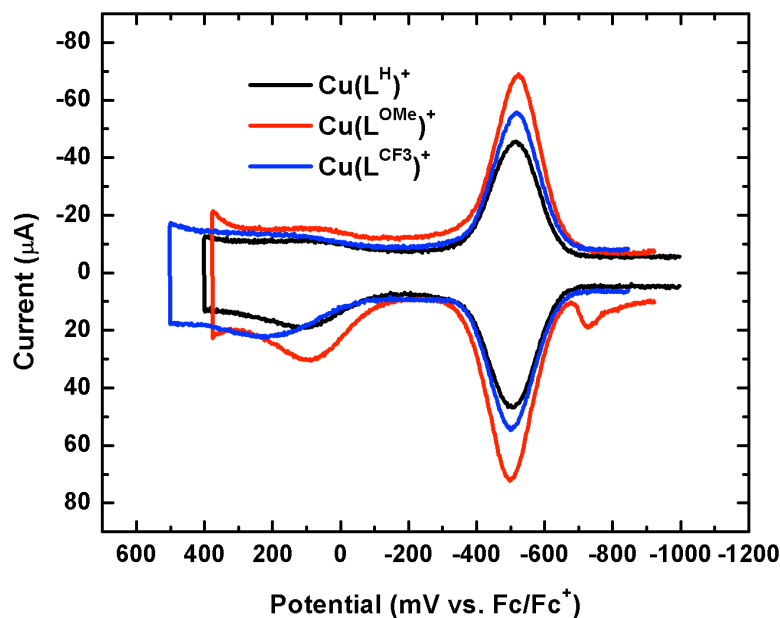


**Figure S27:** Square wave voltammogram of  $[\text{Cu}(\text{L}^{\text{R}})]\text{BAR}'$  ( $\text{R}=\text{H}$ ,  $\text{CF}_3$  and  $\text{OMe}$ ) in 0.1M  $\text{NBu}_4\text{PF}_6$  MeCN with  $\text{Fc}^*$  as internal reference ( $\text{Fc}^*/\text{Fc}^{*+} = -510$  mV vs  $\text{Fc}/\text{Fc}^+$ )

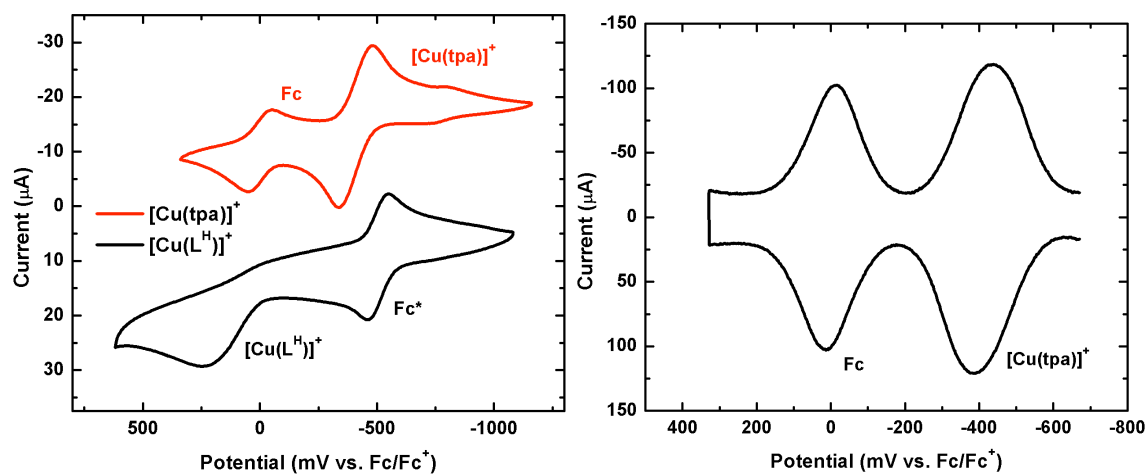


**Figure S28:** Cyclic voltammogram of  $[\text{Cu}(\text{tpa})]\text{BAR}'$  and  $\text{Fc}$  overlaid with  $[\text{Cu}(\text{LH})]\text{BAR}'$  and  $\text{Fc}^*$  (left) and square wave voltammogram of  $[\text{Cu}(\text{tpa})]\text{BAR}'$  with  $\text{Fc}$  internal reference (right). All voltammetry collected in 0.1M  $\text{NBu}_4\text{PF}_6$  MeCN.

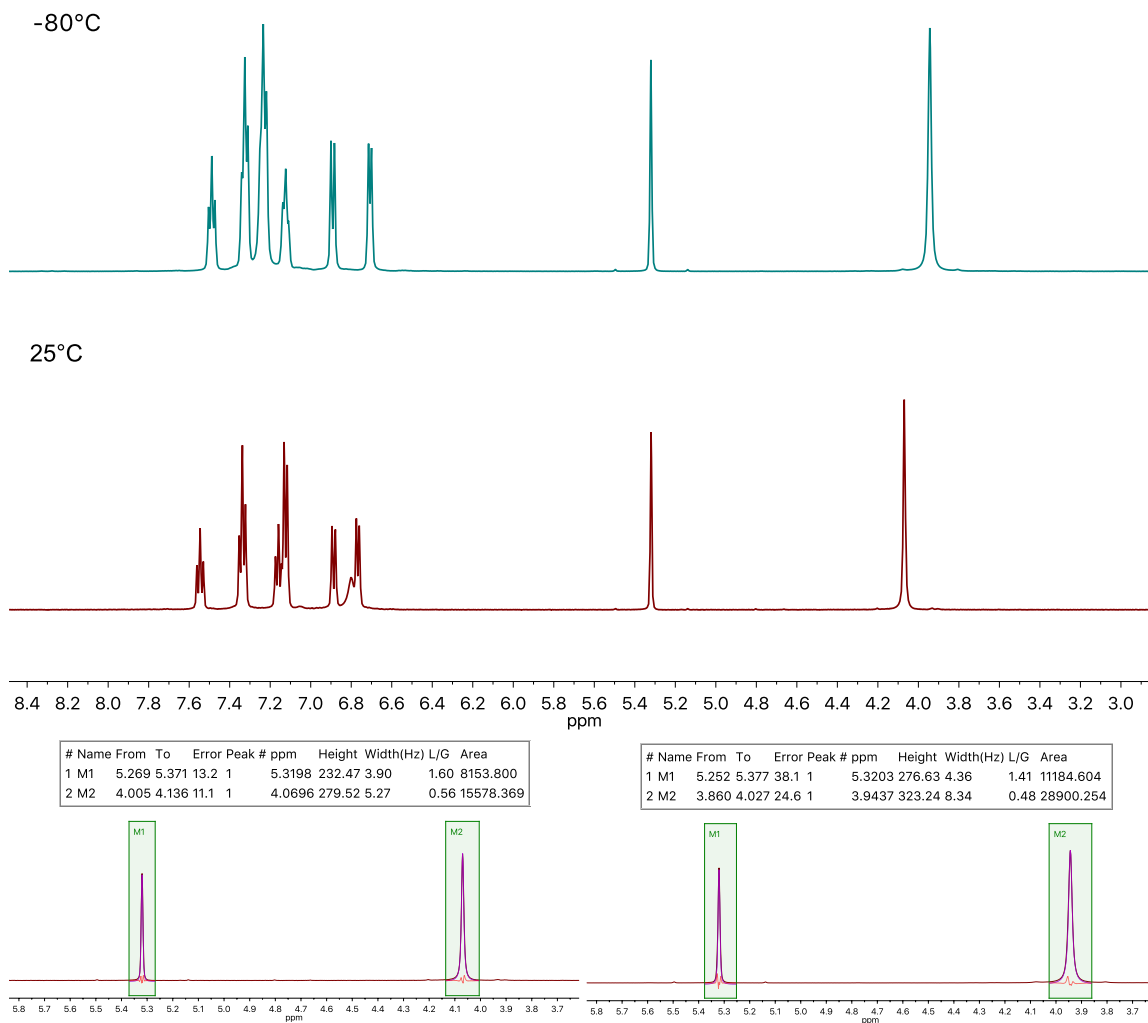


**Figure S29:** Top – Overlay of 500 MHz  $^1\text{H}$  NMR spectra of  $[\text{Cu}(\text{L}^{\text{H}})]\text{BAR}'$  at 25°C and -80°C. Bottom – Line fitting for  $\text{CD}_2\text{Cl}_2$  residual peak and methylene proton peak at 25°C (left) and -80°C (right). Reported peak broadening ( $\Delta\text{fwhm}$ ) was corrected by subtracting the broadening observed for the residual solvent peak (0.46 Hz).

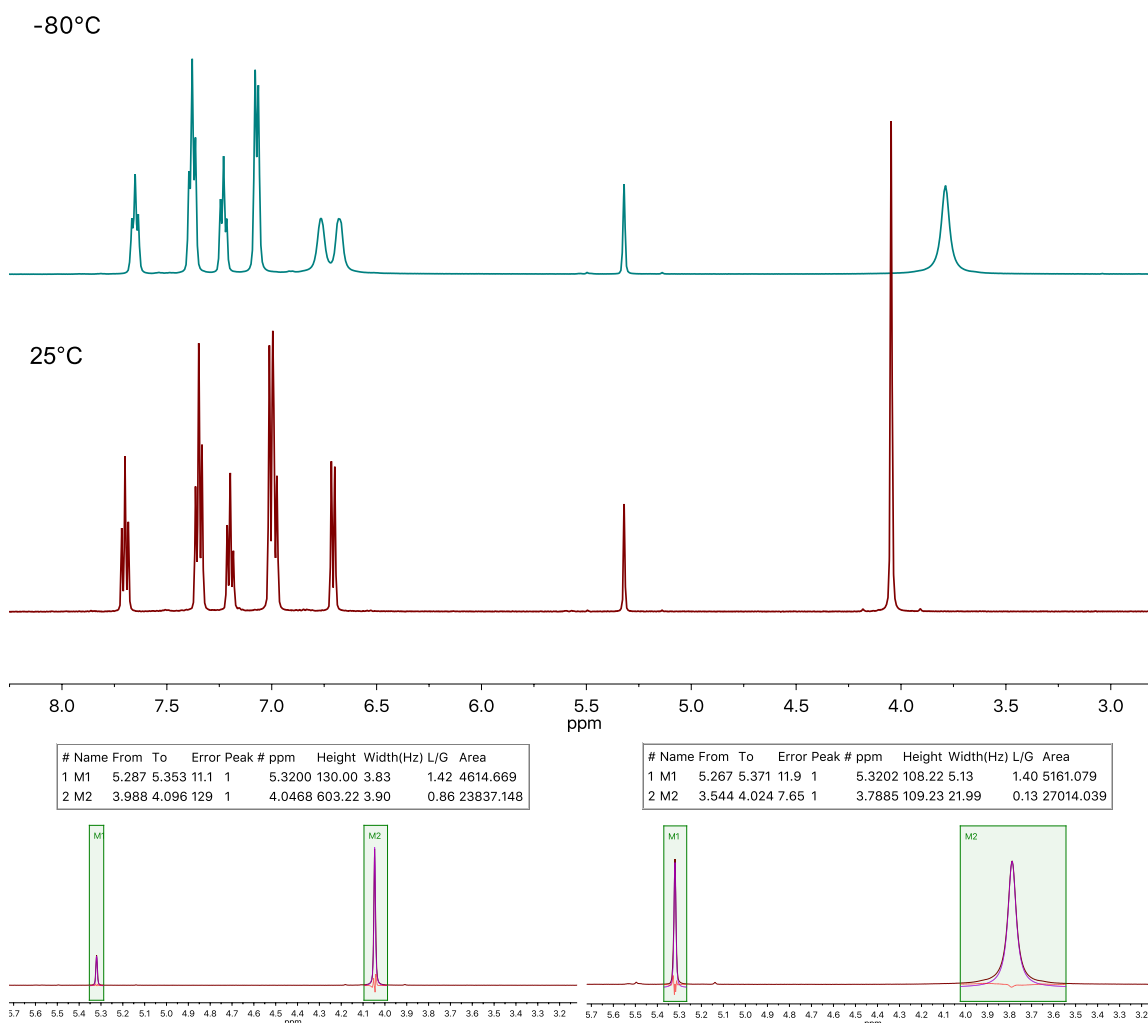


**Figure S30:** Top – Overlay of 500 MHz  $^1\text{H}$  NMR spectra of  $[\text{Cu}(\text{tpa}^{\text{Oph}})]\text{BAR}'$  at 25°C and -80°C. Bottom – Line fitting for  $\text{CD}_2\text{Cl}_2$  residual peak and methylene proton peak at 25°C (left) and -80°C (right). Reported peak broadening ( $\Delta\text{fwhm}$ ) was corrected by subtracting the broadening observed for the residual solvent peak (1.3 Hz).

### Crystallography Details:

Crystals were mounted on a Rigaku AFC10K Saturn 944+ CCD-based X-ray diffractometer with a low temperature apparatus and Micromax-007HF Cu-target micro-focus rotating anode ( $\lambda = 1.54187 \text{ \AA}$ ) operated at 1.2 kW power (40 kV, 30 mA). Samples were measured at 85(2)K. The data were processed with CrystalClear 2.0<sup>4</sup> and corrected for absorption. Structures were solved in Olex2<sup>5</sup> using the XL refinement program<sup>6</sup>.

**Crystal data and structure refinement for 1<sup>H</sup>:**

Identification code	1H
Empirical formula	C <sub>36</sub> H <sub>33</sub> ClCuN <sub>7</sub>
Formula weight	662.68
Temperature/K	85
Crystal system	trigonal
Space group	R-3
a/Å	13.2938(3)
b/Å	13.2938(3)
c/Å	31.3861(8)
α/°	90
β/°	90
γ/°	120
Volume/Å <sup>3</sup>	4803.6(2)
Z	6
ρ <sub>calc</sub> /cm <sup>3</sup>	1.374
μ/mm <sup>-1</sup>	2.021
F(000)	2064.0
Crystal size/mm <sup>3</sup>	0.08 × 0.07 × 0.02
Radiation	CuKα (λ = 1.54184)
2θ range for data collection/°	8.18 to 138.77
Index ranges	-16 ≤ h ≤ 15, -15 ≤ k ≤ 15, -37 ≤ l ≤ 37
Reflections collected	23497
Independent reflections	1987 [R <sub>int</sub> = 0.0568, R <sub>sigma</sub> = 0.0221]
Data/restraints/parameters	1987/0/140
Goodness-of-fit on F <sup>2</sup>	1.063
Final R indexes [I ≥ 2σ (I)]	R <sub>1</sub> = 0.0603, wR <sub>2</sub> = 0.1591
Final R indexes [all data]	R <sub>1</sub> = 0.0676, wR <sub>2</sub> = 0.1667
Largest diff. peak/hole / e Å <sup>-3</sup>	0.74/-0.82

**Crystal data and structure refinement for 2<sup>H</sup>:**

Identification code	2H
Empirical formula	C <sub>62</sub> H <sub>37</sub> BCl <sub>4</sub> CuF <sub>20</sub> N <sub>7</sub> O
Formula weight	1492.13
Temperature/K	85
Crystal system	triclinic
Space group	P-1
a/Å	13.7619(9)
b/Å	14.9539(9)
c/Å	16.6243(7)
α/°	106.175(5)
β/°	102.188(5)
γ/°	107.466(6)
Volume/Å <sup>3</sup>	2967.6(3)
Z	2
ρ <sub>calc</sub> /cm <sup>3</sup>	1.670
μ/mm <sup>-1</sup>	3.204
F(000)	1496.0
Crystal size/mm <sup>3</sup>	0.14 × 0.03 × 0.03
Radiation	CuKα (λ = 1.54184)
2θ range for data collection/°	5.846 to 139.664
Index ranges	-16 ≤ h ≤ 16, -18 ≤ k ≤ 18, -20 ≤ l ≤ 19
Reflections collected	43076
Independent reflections	10724 [R <sub>int</sub> = 0.1048, R <sub>sigma</sub> = 0.0724]
Data/restraints/parameters	10724/3/877
Goodness-of-fit on F <sup>2</sup>	1.116
Final R indexes [I ≥ 2σ (I)]	R <sub>1</sub> = 0.0885, wR <sub>2</sub> = 0.2417
Final R indexes [all data]	R <sub>1</sub> = 0.1117, wR <sub>2</sub> = 0.2918
Largest diff. peak/hole / e Å <sup>-3</sup>	0.89/-1.28

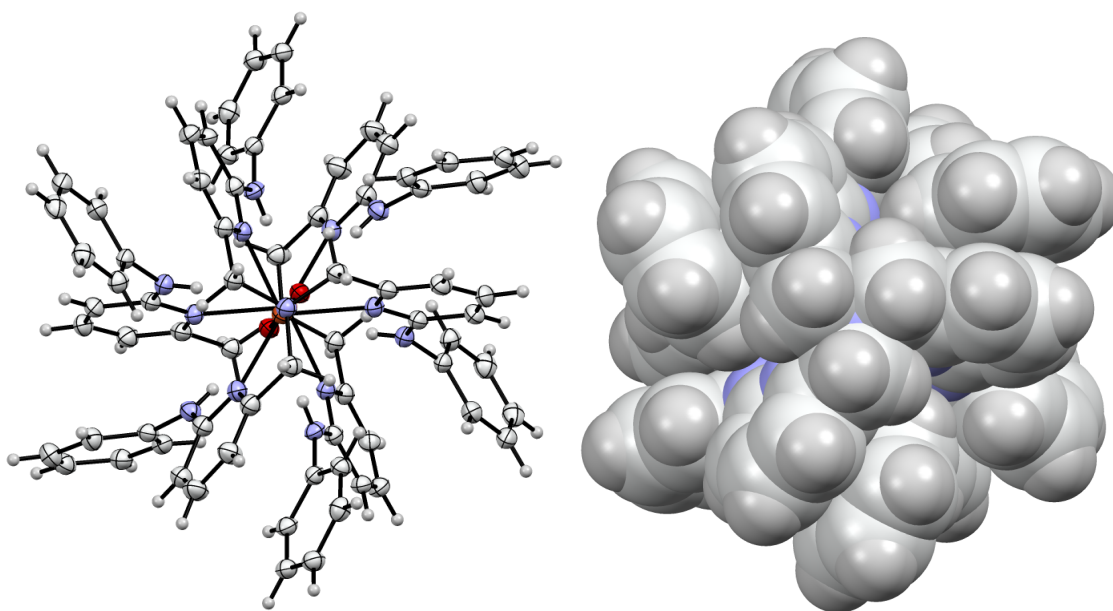


**Figure S31:** ORTEP (left) and space-filling model (right) of **2<sup>H</sup>** to show steric protection of peroxo unit.

#### References:

- 1) C.-L. Chuang, O. dos Santos, X. Xu, J. W. Canary. *Inorg. Chem.* **1997**, 36, 1967-1972.
- 2) H.-C. Liang, E. Kim, C. D. Incarvito, A. L. Rheingold, K. D. Karlin. *Inorg. Chem.* **2002**, 41, 2209-2212.
- 3) L. Lochmann, J. Pospíšil, D. Lím, *Tetrahedron Lett.* **1966**, 257.
- 4) CrystalClear Expert 2.0 r12, Rigaku Americas and Rigaku Corporation (2011), Rigaku Americas, 9009, TX, USA 77381-5209, Rigaku Tokyo, 196-8666, Japan.
- 5) O. V. Dolomanov, L. J. Bourhis, R. J. Gildea, J. A. K. Howard and H. Puschmann. *J. Appl. Cryst.* **2009**, 42, 339-341.
- 6) G. M. Sheldrick, *Acta Cryst. A* **2008**, 64, 112-122.